Electronic Supplementary Information for

Alginate-oligothiophenes aerogels as photocatalysts for degradation of emerging organic contaminants in water

Andrea Trifoglio,[a,c] ‡Francesca Tunioli,[a,c] ‡ Laura Favaretto,[a] Massimo Zambianchi,[a] Cristian Bettini,[a] Ilse Manet, [a] Livia Mariani,[b] Anna Barra Caracciolo,[b] Paola Grenni,[b] Manuele Di Sante,[c,d] Matteo Di Giosia,[c,d] Tainah Dorina Marforio,[c,d] Edoardo Jun Mattioli,[c,d] Matteo Calvaresi, [c,d,*] Manuela Melucci[a, *]

[a] Institute for Organic Synthesis and Photoreactivity (ISOF), National Research Council of Italy (CNR), Via P. Gobetti 101, 40129 Bologna, Italy.
[b] Water Research Institute (IRSA), Via Salaria Km 29,300 C.P. 10 - 00015 Monterotondo Stazione Rome, Italy
[c] Department of Chemistry 'G. Ciamician', Alma Mater Studiorum – University of Bologna, Via Selmi 2, 40126 Bologna, Italy
[d] IRCCS Azienda Ospedaliero - Universitaria di Bologna, - Preclinical & Translational Research in Oncology lab (PRO), Bologna, Italy.

1. Materials synthesis and characterization

1.1 Synthesis of BT molecules

*2,3-Dibromobenzo[b]thiophene-1-oxide (**2**).* To a solution of commercial 2,3-dibromo-benzo[*b*]thiophene **(1)** (0.5 mmol, 0.15 g) in 6 mL of CH_2Cl_2 was added dropwise at -20 °C the $BF_3.Et_2O$ (9 eq, 4.5 mmol, 0.57 mL). After 15 min, the temperature was adjusted at -40 °C and mCPBA (70 wt.%, 1.2 eq, 0.6 mmol, 0.15 g) was added stepwise. The mixture was left stirring for 2 h at this temperature before washing with saturated Na_2CO_3 aq. (20 mL), then with deionized (DI) water (2 x 20 mL). After drying over anhydrous Na_2SO_4, the solvent was removed in vacuum and the residue was chromatographed over silica gel using pentane/CH_2Cl_2/EA 70:15:15 (v/v) as the eluent. A microcrystalline white solid was obtained (0.12 g, 76% yield); m.p. 155 °C; GC-EI-MS *m/z* 292 [M•$^+$]; λ_{max} = 326 nm in CH_2Cl_2. ^{1}H NMR ($CDCl_3$, TMS/ppm) δ 7.86 (m, 1H), 7.56 (m, 3H); ^{13}C NMR ($CDCl_3$, TMS/ppm) δ 143.6, 136.7, 132.9, 131.3, 129.8, 128.8, 126.3, 124.3.

*5-(Trimethylstannyl)-2,2'-bithiazole (**6**).* *n*-BuLi (2.5 M in hexane, 1.1 eq, 6.6 mmol, 2.64 mL) was added dropwise to a solution of 1.0 g (6.0 mmol) of 2,2-bithiazole in 50 mL of THF at -70 °C and the mixture was stirred for 40 min. Afterwards, Me_3SnCl (1.1 eq, 6.6 mmol, 1.32 g) was added dropwise, then the solution was allowed to reach room temperature and stirred overnight. 20 mL of a saturated solution of NH_4Cl aq. was then added; the organic layer was washed with DI water (2 x 50 mL), dried over Na_2SO_4, and evaporated. The obtained crude (1.89 g) was a mixture of the title product and unreacted starting 2,2-bithiazole (85:15 ratio respectively), which was used without further purification step for the next reaction. DEP-EI-MS *m/z* 335 [M•$^+$]; ^{1}H NMR ($CDCl_3$, TMS/ppm) δ 7.89 (d, *J* = 3.2 Hz, 1H), 7.81 (s, 1H), 7.41 (d, *J* = 3.2 Hz, 1H), 0.46 (s, 9H).

*2-Bromo-3-methylbenzo[b]thiophene (**11**).* Under exclusion of light, NBS (0.008 mol, 1.4 g) was added stepwise to a solution of commercial 3-methylbenzothiophene **(10)** (0.0068 mol, 1 g) in 40 mL of acetic acid/CH_2Cl_2 1:1 (v/v) at 0 °C. After overnight stirring, the mixture was washed with saturated KOH aq. (2 x 30 mL), saturated $NaHCO_3$ aq. (2 x 30 mL), then with DI water (2 x 30 mL). The solvent was removed under reduced pressure. The obtained residue (yellow-orange oil) was used for the following reaction without purification. Yield 100%; GC-EI-MS *m/z* 228 [M•$^+$]; ^{1}H NMR ($CDCl_3$, TMS/ppm) δ 7.72 (m, 1H), 7.62 (m, 1H), 7.33 (m, 2H), 2.37 (s, 3H); ^{13}C NMR ($CDCl_3$, TMS/ppm) δ 139.6, 138.6, 131.7, 124.5, 124.4, 121.7, 121.6, 112.4, 13.1.

*2-Bromo-3-methylbenzo[b]thiophene-1,1-dioxide (**12**).* A solution of **11** (0.0048 mol, 1.1 g) in 8 mL of methylene chloride was added dropwise to a solution of mCPBA (70 wt.%, 2.5 eq, 0.012 mol, 3 g) in 25 mL of CH_2Cl_2 and the mixture stirred overnight. Afterwards the mixture was washed with saturated KOH aq. (2 x 20 mL), saturated $NaHCO_3$ aq. (2 x 20 mL), then with DI water (2 x 20 mL), dried over Na_2SO_4, and evaporated. After crystallization from CH_2Cl_2, 1.1 g of a microcrystalline white solid were obtained: 90% yield; m.p. 140 °C; GC-EI-MS *m/z* 260 [M•$^+$]; λ_{max} = 315 nm in CH_2Cl_2. ^{1}H NMR ($CDCl_3$, TMS/ppm) δ 7.77 (m, 1H), 7.60 (m, 1H), 7.52 (m, 1H), 7.44 (m, 1H), 2.26 (s, 3H); ^{13}C NMR ($CDCl_3$, TMS/ppm) δ 138.8, 135.7, 133.9, 133.0, 129.9, 122.0, 121.7, 119.4, 12.9.

*2-([2,2'-Bithiophen]-5-yl)-3-methylbenzo[b]thiophene-1,1-dioxide (**13**).* A solution of $Pd_2(dba)_3{\cdot}CHCl_3$ (0.05 mmol, 51.8 mg) and $AsPh_3$ (0.4 mmol, 122.4 mg) in 90 mL of toluene under a nitrogen stream was warmed to reflux, then 0.65 g (2.5 mmol) of compound **12** in 12 mL of toluene was added to the mixture. Afterwards, 1.25 g (1.1 eq, 2.75 mmol) of compound (**3**)[1] in 10 mL of toluene was added dropwise and the mixture stirred for 5 h. The solvent was evaporated and the crude product was purified *via* column chromatography (silica gel, pentane/acetone/EA 80:10:10 v/v). The isolated product was recrystallized from toluene and pentane to obtain a yellow powder (0.78 g, 91%

yield); m.p. 180 °C; DEP-EI-MS *m/z* 344 [M•$^+$]; λ_{max} = 395 nm in CH_2Cl_2; λ_{PL} = 487 nm in CH_2Cl_2. ^{1}H NMR ($CDCl_3$, TMS/ppm) δ 7.79 (m, 1H), 7.63 (m, 2H), 7.51 (m, 2H), 7.29 (dd, *J* = 5.2, 1.2 Hz, 1H), 7.26 (m, 2H), 7.06 (dd, *J* = 5.2, 3.6 Hz, 1H), 2.49 (s, 3H); ^{13}C NMR ($CDCl_3$, TMS/ppm) δ 140.6, 136.3, 135.7, 133.8, 133.7, 132.3, 131.8, 129.9, 129.6, 128.0, 127.0, 126.5, 124.7, 124.3, 122.2, 121.2, 12.5.

*2-(5'-Bromo-[2,2'-bithiophen]-5-yl)-3-methylbenzo[b]thiophene 1,1-dioxide (**14**).* Under dark conditions, NBS (1.1 eq, 1.32 mmol, 0.23 g) was added stepwise to a solution of compound **13** (1.20 mmol, 0.41 g) in 12 mL of acetic acid/ CH_2Cl_2 6:4 (v/v) at room temperature. After overnight stirring CH_2Cl_2 (10 ml) was added to dissolve the precipitate. The mixture was washed with 20% KOH aq. (2 x 20 mL), saturated $NaHCO_3$ aq. (2 x 20 mL), then with DI water (2 x 20 mL). After drying over anhydrous Na_2SO_4 the solvent was removed under reduced pressure. The obtained residue was used for the following reaction without purification. Yellow-orange powder (0.51 g, 100% yield); m.p. 157 °C; DEP-EI-MS *m/z* 424 [M•$^+$]; λ_{max} = 396 nm in CH_2Cl_2. ^{1}H NMR ($CDCl_3$, TMS/ppm) δ 7.77 (m, 1H), 7.62 (m, 2H), 7.51 (m, 2H), 7.18 (d, *J* = 4 Hz, 1H), 7.00, (s, 2H), 2.46 (s, 3H); ^{13}C NMR ($CDCl_3$, TMS/ppm) δ 139.3, 137.7, 135.7, 133.8, 133.6, 132.3, 132.2, 130.9, 129.9, 129.7, 127.4, 124.8, 124.5, 122.3, 121.2, 112.4, 12.5.

*3-Methyl-2-(5'-(tributylstannyl)-[2,2'-bithiophen]-5-yl)benzo[b]thiophene-1,1-dioxide (**8**).* *n*-BuLi (2.5 M in hexane, 1.15 eq, 1.38 mmol, 0.55 mL) was added dropwise to a solution of compound **14** (1.20 mmol, 0.51 g) in 16 mL of THF at -70 °C. The mixture was stirred at -70 °C for 1 h and at -40 °C for a further 30 min. After lowering the temperature at -70 °C, Bu_3SnCl (1.15 eq, 1.38 mmol, 0.37 mL) was added dropwise, then the solution was allowed to reach room temperature and stirred overnight. After removal of the solvent by using a rotary evaporator, the residue was dissolved in CH_2Cl_2 (20 mL), washed in DI water (2 x 20 mL), and evaporated. A silica gel-packed column (pretreated with trimethylamine) was used for the separation of the title product with pentane/acetone/CH_2Cl_2 80:10:10 v/v as the eluent. Thick yellow oil (0.39 g, 51% yield): DEP-EI-MS *m/z* 634 [M•$^+$]; ^{1}H NMR ($CDCl_3$, TMS/ppm) δ 7.58 (m, 1H), 7.66 (d, *J* = 4 Hz, 1H), 7.59 (m, 1H), 7.48 (m, 2H), 7.38 (d, *J* = 3.6 Hz, 1H), 7.25, (d, *J* = 4 Hz, 1H), 7.11 (d, *J* = Hz, 1H), 2.46 (s, 3H), 1.60 (m, 6H), 1.37 (m, 6H), 1.15 (m, 6H), 0.93 (s, 9H); ^{13}C NMR ($CDCl_3$, TMS/ppm) δ 141.5, 140.8, 138.6, 136.3, 135.6, 133.7, 132.4, 131.2, 129.9, 129.4, 126.6, 125.8, 123.9, 122.1, 121.0, 28.9, 27.2, 13.6, 12.5, 10.9.

1.2 Characterization of BT molecules and alginate aerogels

All ^{1}H NMR, and ^{13}C NMR spectra were recorded at room temperature on a Varian Mercury-400 spectrometer (Varian, Palo, Alto, CA, USA) equipped with a 5-mm probe. For ^{1}H NMR spectra chemical shifts are reported in ppm from tetramethylsilane as an internal standard. Data are reported as follows: chemical shift, multiplicity, coupling constants (Hz), and integration. ^{13}C-NMR spectra were recorded with complete proton decoupling. Chemical shifts are reported in ppm from the residual solvent as an internal standard. Mass spectra were determined using a Trace 1300 gas chromatograph or employing the direct exposure probe (DEP) tool, and ISQ EI mass spectrometer (Thermo Fisher Scientific, Waltham, MA, USA). UV-VIS spectra were recorded using a Cary 3500 spectrometer (Agilent Technologies, Santa Clara, CA, USA). Photoluminescence spectra were obtained with a LS50 spectrofluorometer (PerkinElmer, Waltham, MA, USA). Fluorescence measurements were made at an excitation wavelength corresponding to the maximum absorption lambda. Melting points are uncorrected. Melting processes were observed on a Leica DM LS optical microscope equipped with a Leica 350 heating stage (Leica Microsystems, Wetzlar, Germany). SEM

was performed by using Environmental Scanning Electron Microscope Zeiss EVO LS 10 LaB6 operated at 15 kV. Samples were coated by gold prior measurement.

1.3 BTs photophysical data

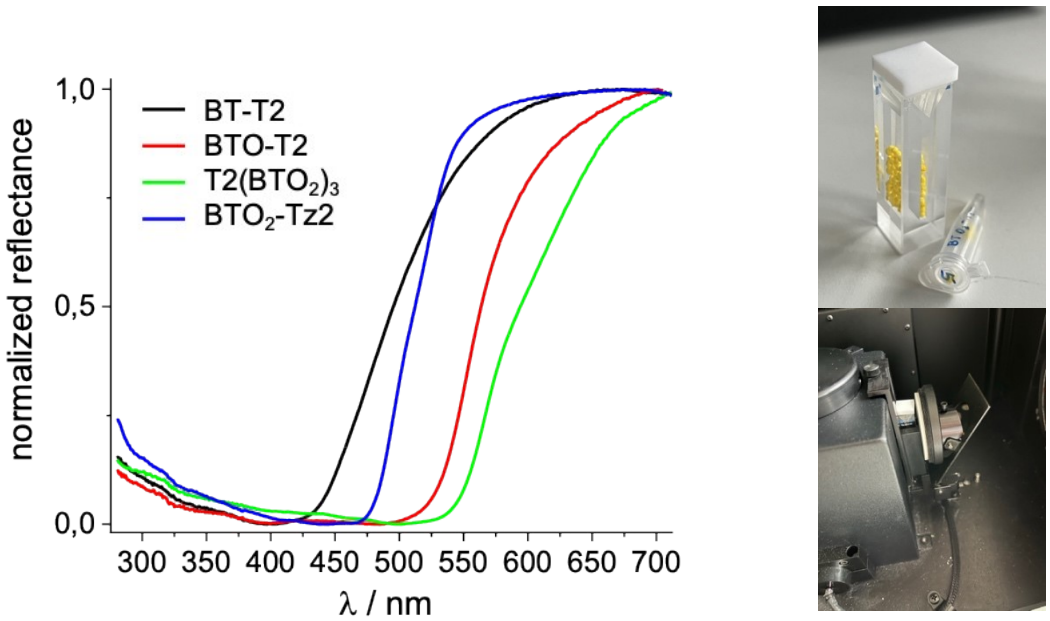

Figure S1: Reflectance spectra of the beads collected in quartz cuvet with 2 mm optical depth and 10 mm width.

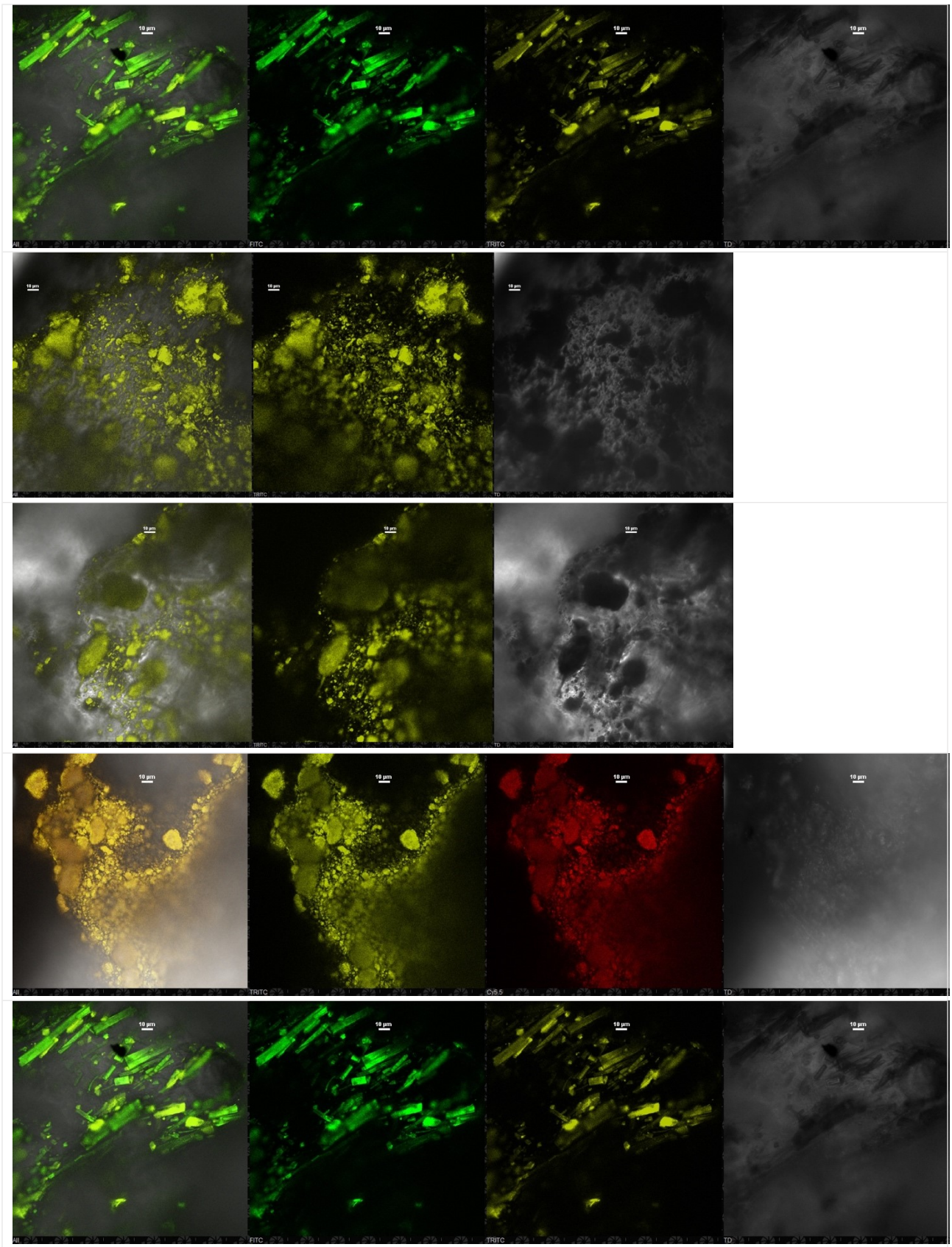

Figure S2a: Fluorescence intensity and DIC Images of the beads: from top to bottom BT-T2, BTO-T2, BTO_2-T2, T2$(BTO_2)_3$ and BTO_2-Tz2: left image is overlay of DIC image (right) with the fluorescence intensity images in the green, yellow, or red ranges. Scale bar corresponds to 10 μm.

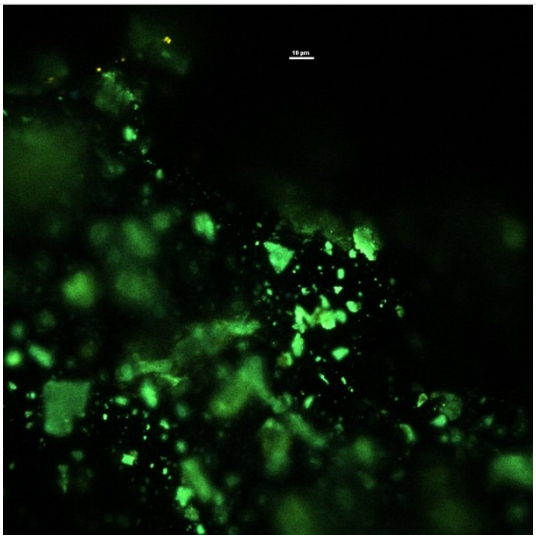

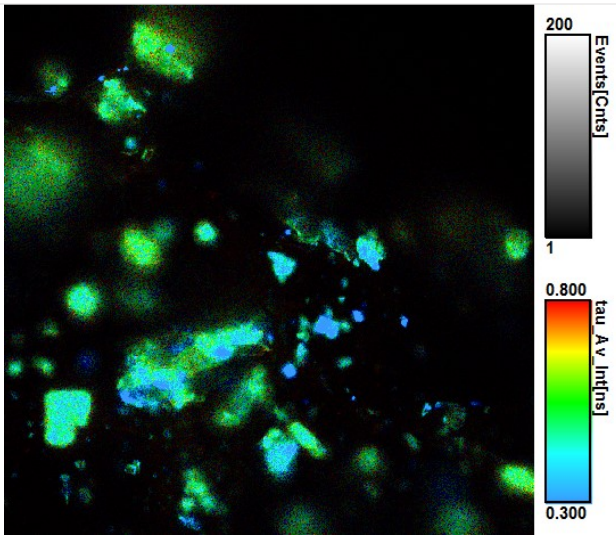

525±25nm

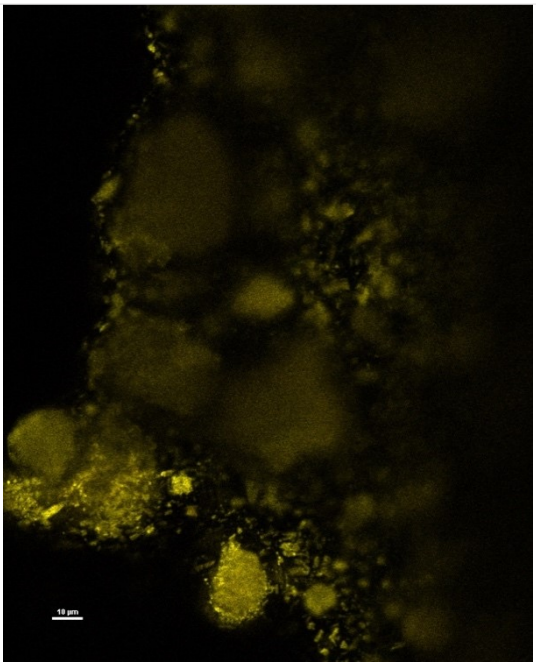

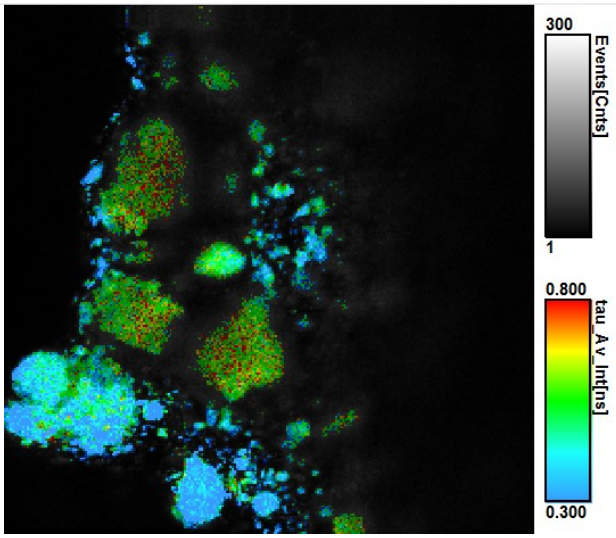

585±25 nm

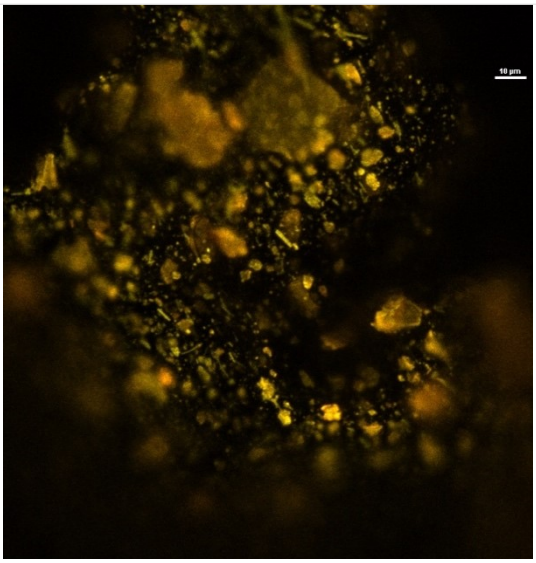

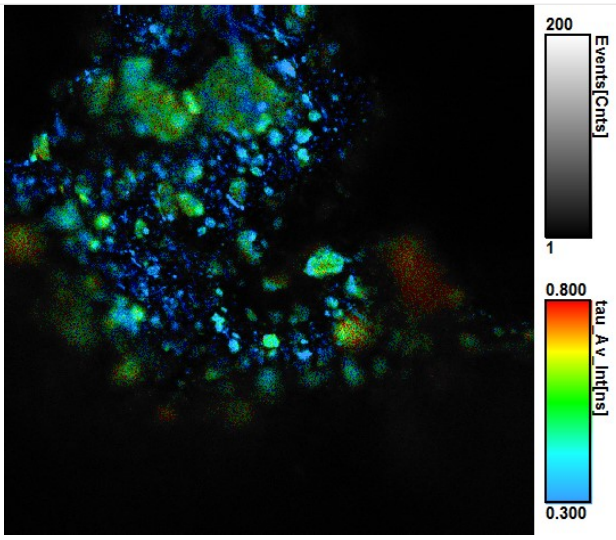

585±25 nm

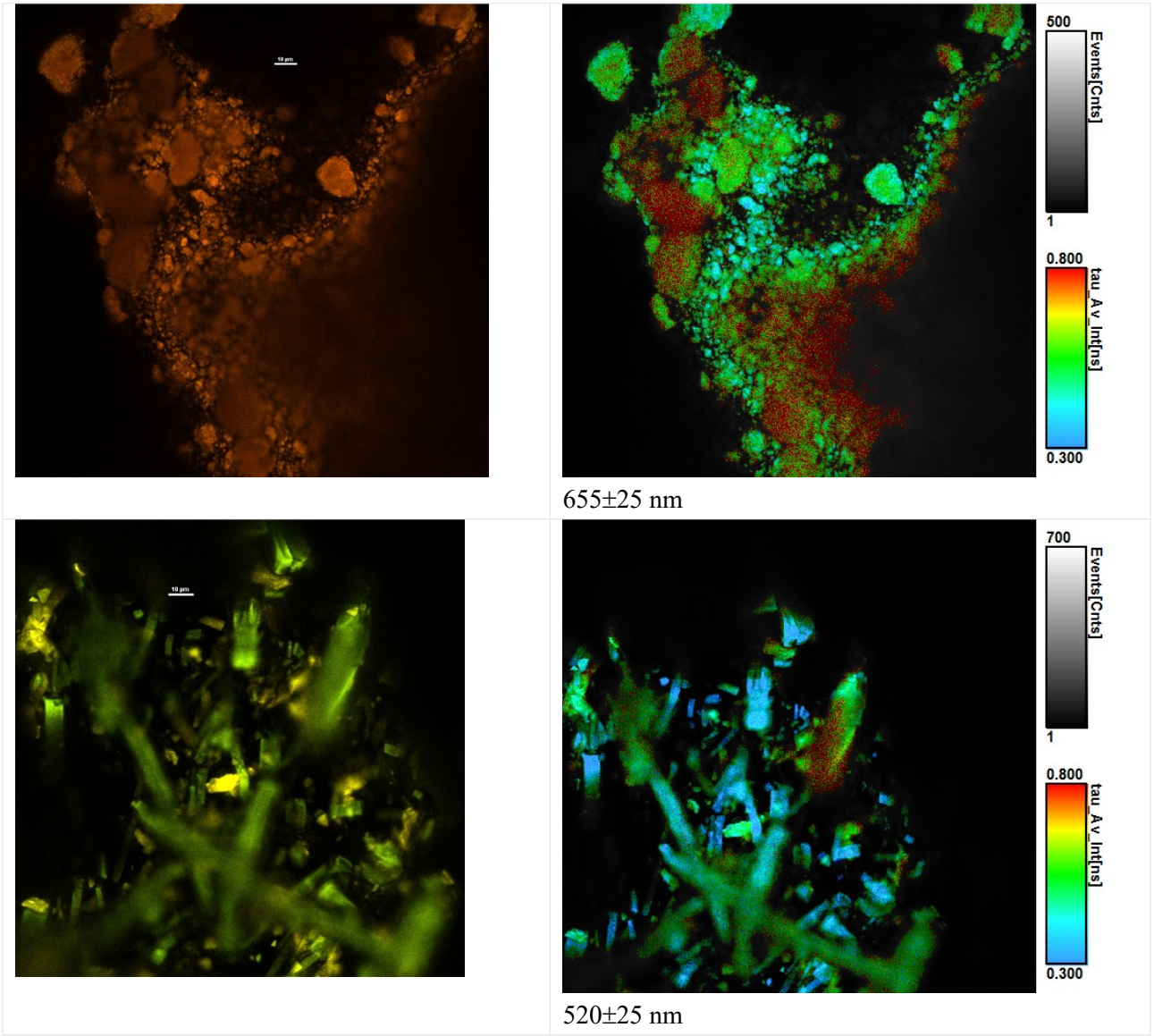

Figure S2b: Confocal spectral (left) images and FLIM (right) images representing the average fluorescence lifetime in color scale ranging from 0,3 to 0,8 ns (emission wavelength range is indicated below the image); from top to bottom: beads with BT-T2, BTO-T2, BTO_2-T2, $T2(BTO_2)_3$ and BTO_2-Tz2. Excitation at 488 nm (spectral image) and 485 nm (FLIM) except for BT-T2 excited at 405 nm. 60X oil-immersion objective (NA 1,4). Scale bar corresponds to 10 μm.

Table S1. Fluorescence lifetimes obtained fitting with a bi-exponential decay function a region of interest in the image and used to calculate the average fluorescence lifetime image in Figure S2b.

	τ_1	τ_2
BT-T2	0,3 ns	1,2 ns
BTO-T2	0,3 ns	1,2 ns
BTO_2-T2	0,3 ns	1,1 ns
$T2(BTO_2)_3$	0,3 ns	1,4 ns
BTO_2-TZ2	0,25 ns	0,7 ns

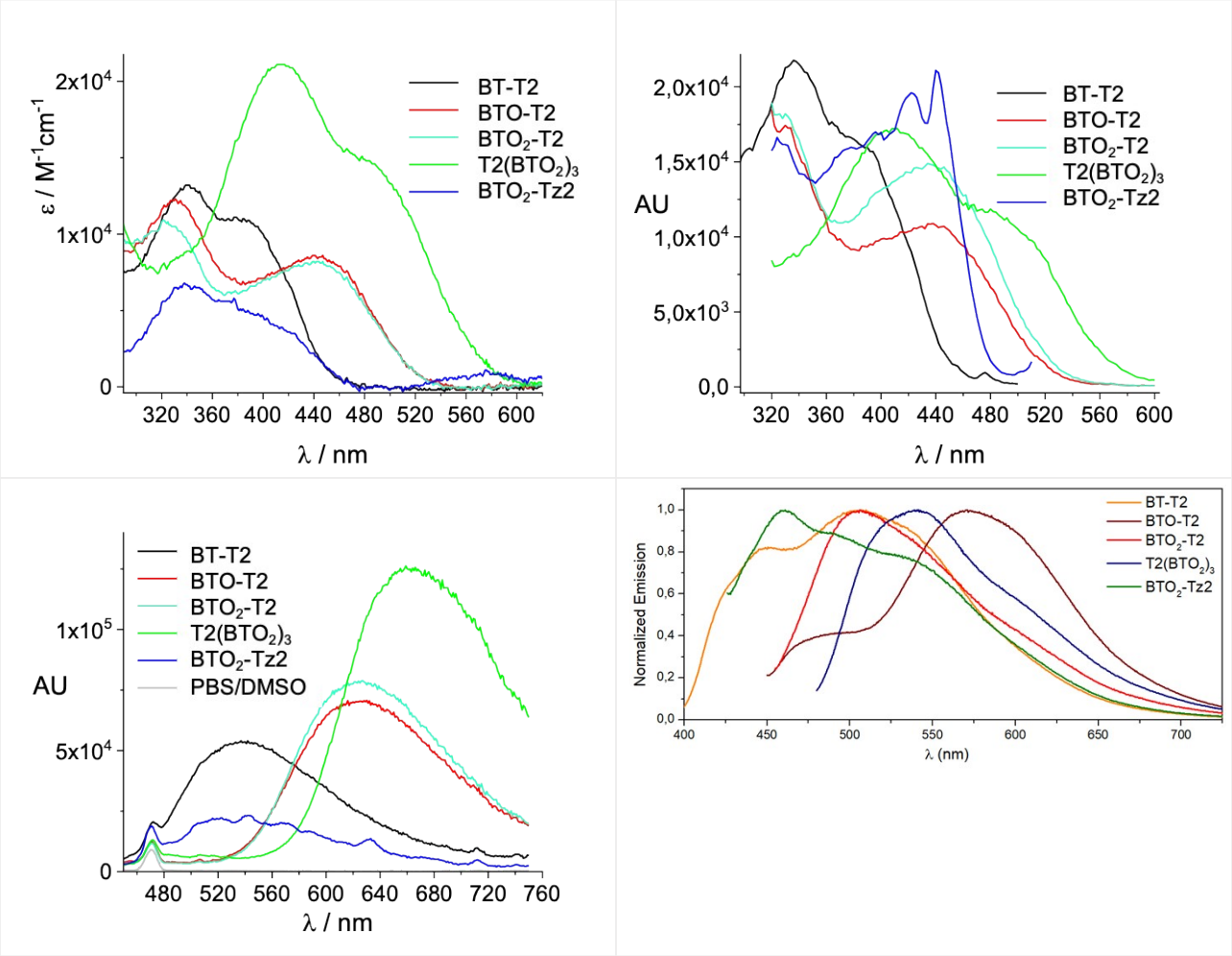

Figure S3. Absorption, excitation and fluorescence spectra of 1 μM BT-T2, BTO-T2, BTO_2-T2, $T2(BTO_2)_3$ and BTO_2-Tz2 in PBS/DMSO and fluorescence spectra of BT-T2, BTO-T2, BTO_2-T2, $T2(BTO_2)_3$ and BTO_2-Tz2 in CH_2Cl_2.

2. Theoretical calculations

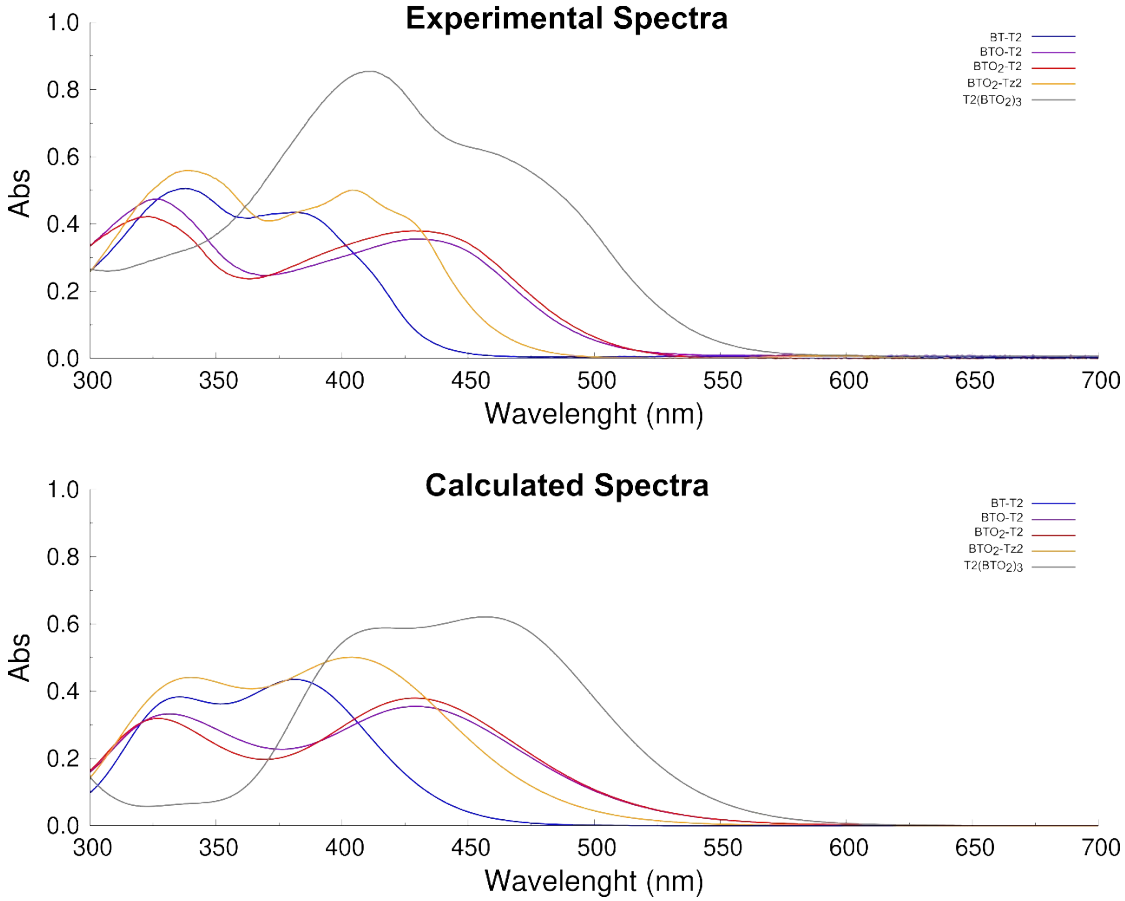

Figure S4. On top. Experimental spectra of BT-T2, BTO-T2, BTO_2-T2, BTO_2-Tz2 and, $T2(BTO_2)_3$. On bottom. Calculated spectra of BT-T2, BTO-T2, BTO_2-T2, BTO_2-Tz2 and, $T2(BTO_2)_3$.

Table S2. Excited singlet state S_1 energy, oscillator strength, MOs involved in the $S_0 \rightarrow S_1$ transition and, triplet state T_1 energy for compounds BT-T2, BTO-T2, BTO_2-T2, $T2(BTO_2)_3$ and BTO_2-Tz2.

Structure	S1 (nm)	S1 (eV)	Extinction coefficient (ε) ($M^{-1} \cdot cm^{-1}$)	f	Trs	T1 (eV)
BT-T2	359	3.45	21748	0.903	H->L	2.07
BTO-T2	406	3.06	17756	0.739	H->L	1.57
BTO_2-T2	405	3.06	18979	0.790	H->L H-2->L	1.51
$T2(BTO_2)_3$	421	2.95	42718	1.348	H->L H-2->L+2	1.50
BTO_2-Tz2	386	3.21	25054	0.817	H->L H-2->L+2	1.68

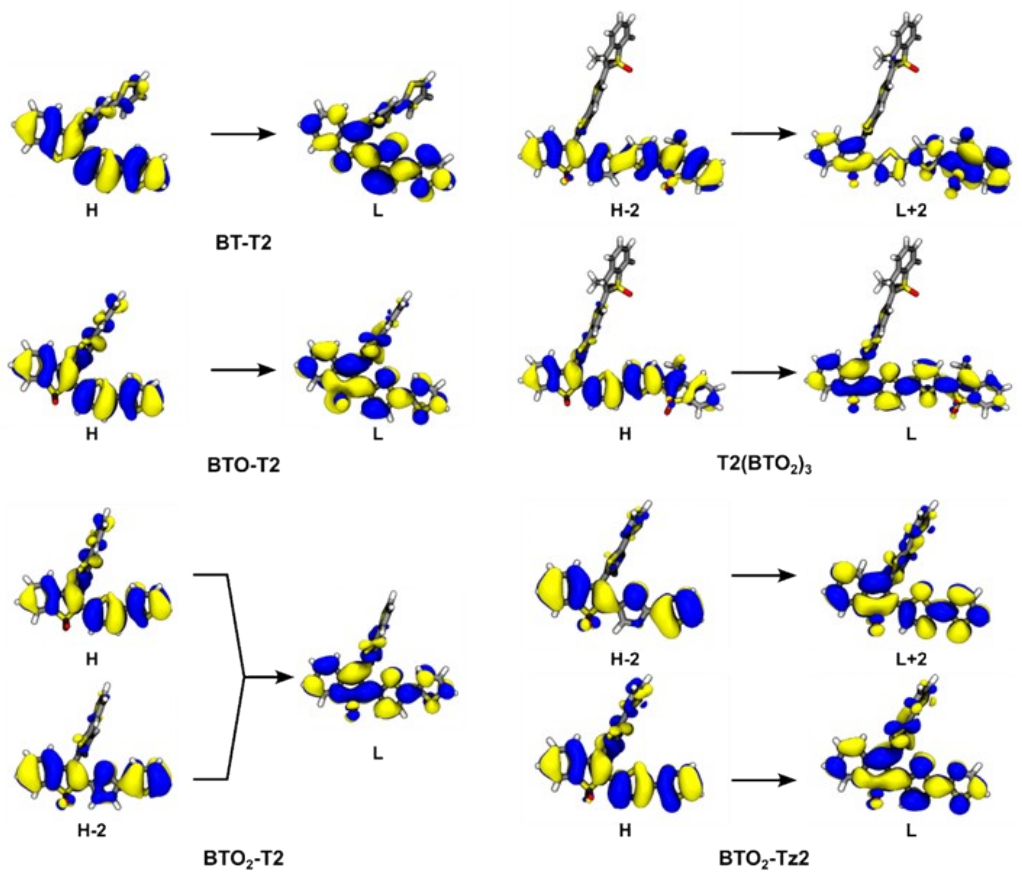

Figure S5. MOs (H = HOMO, L = LUMO) involved in $S_0 \rightarrow S_1$ transition for BT-T2, BTO-T2, BTO_2-T2, $T2(BTO_2)_3$ and, BTO_2-Tz2.

Table S3: Average fluorescence lifetime of the oligothiophenes in solution for excitation at 405 nm.

	PBS-DMSO	**DMSO**
BT-T2	0,22 ns	0,34 ns
BTO-T2	0,68 ns	0,62 ns
BTO_2-T2	0,56 ns	0,58 ns
$T2(BTO_2)_3$	0,31 ns	0,26 ns
BTO_2-Tz2	0,21 ns	0,08 ns

BT-T2, exc. at 405 nm	BT-T2, exc. at 488 nm

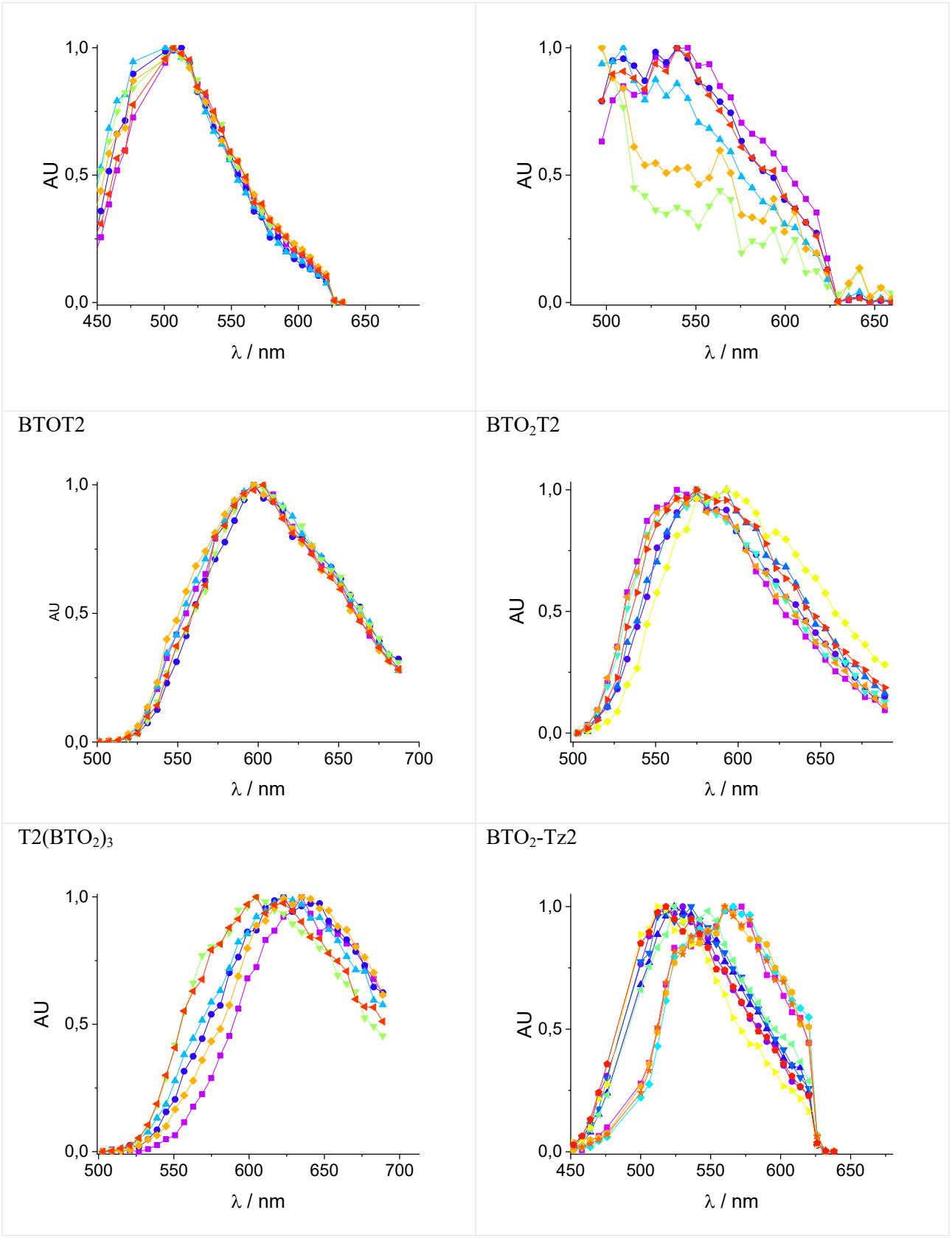

Figure S6: Confocal normalized spectra calculated for selected regions of interest in the images in Figure S2. Excitation at 488 nm unless otherwise noted.

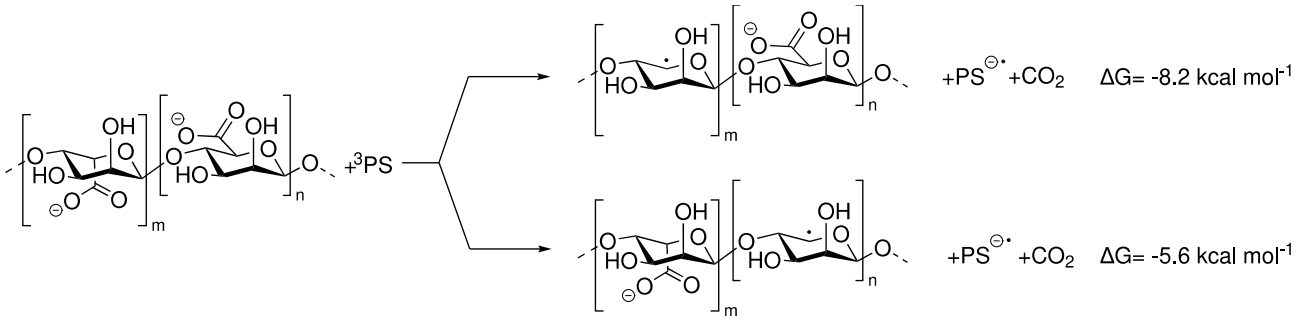

Figure S7. Mechanism for the formation of the thiophene anion radical in the case of BTO_2-Tz2 inside the alginate beads.

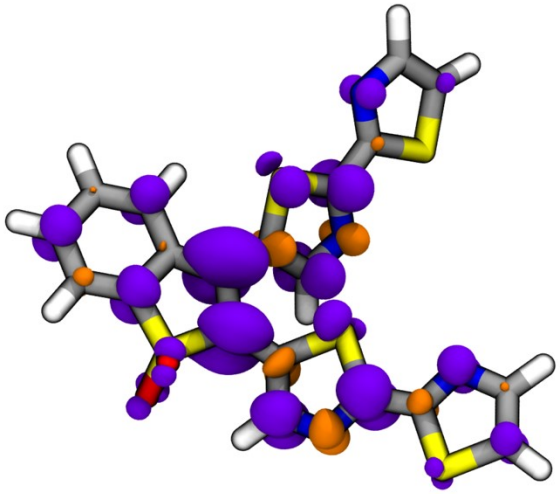

Figure S8. Spin density map of the BTO_2-Tz2 anion radical.

3. Light-induced Reactive Oxygen Species quantification

Amplex Red assay. The concentration of peroxides produced by irradiating the oligothiophenes was estimated through the Amplex Red assay. This test is based on the enzymatic-catalyzed oxidation of nonfluorescent Amplex Red by peroxides, producing fluorescent resorufin (Figure 5b).[10-13] To perform this test, two 96-multiwell plates were used, loading 90 µL of each oligothiophene sample (PBS, 5% DMSO) 1 µM into each well. While one plate was maintained in the dark, the other plate was irradiated 60 minutes using a blue LED (irradiance 10 mW cm^{-2}, energy fluence = 36 J cm^{-2}, measured with the photo-radiometer Delta Ohm LP 471 RAD on the plate surface). A freshly prepared working solution (WS) was produced by mixing HRP enzyme (0.4 µg/mL) and Amplex Red (500 µM) in 50 mM phosphate buffer. Following the addition of 10 µL of the WS to each well, both plates were incubated for 30 minutes in the dark at room temperature. The calculation of the generation of peroxides by alginate-BT aerogels was carried out with the same conditions, by inserting a single bead into 200 µL of phosphate buffer, irradiating and then loading 90 µL of the solution into each well with 10 µL of the WS. Using the EnSpire® Multimode Plate Reader (PerkinElmer), the emission intensity of the resorufin, corrected taking in account the emission contribution of thiophenes to resorufin signal, was recorded at 590 nm (λ_{ex} 530 nm) to estimate the total amount of generated peroxides. A calibration curve made with H_2O_2 standard solutions was used

to convert the fluorescence signal into the H_2O_2 concentration. Each condition was examined in triplicates, and the standard deviation was calculated.

ABMDMA assay. The amount of singlet oxygen ($^1O_2$) produced by the oligothiophenes after light irradiation was estimated by using the ABMDMA assay. The selective reaction between the ABMDMA molecule and the singlet oxygen breaks the conjugation of the anthracene moiety, producing a stable endoperoxide (Figure 5a) that is transparent in the ABMDMA absorption range. The decrease of the ABMDMA absorbance is used to estimate the amount of singlet oxygen produced.[14-17] To prevent the quenching of the singlet oxygen by H_2O, each oligothiophene stock solution (in DMSO) was diluted with deuterated PBS to obtain a final concentration of 1 µM. A 96-multiwell plate was loaded with 97 µL of each solution (1 µM) and mixed with 3 µL of ABMDMA (5 mM) in DMSO. The calculation of the generation of singlet oxygen by alginate-BT aerogels was carried out with same conditions, by inserting a single bead into 200 µL of deuterated PBS (ABMDMA 150 µM). Successively, the plate was irradiated using the same conditions of the Amplex Red assay. Using an EnSpire® Multimode Plate Reader (PerkinElmer, Waltham, MA, USA), the absorbance was recorded at 380 nm, before and after the irradiation. Each condition was examined in triplicates, and the standard deviation was calculated.

4. Photodegradation experiments

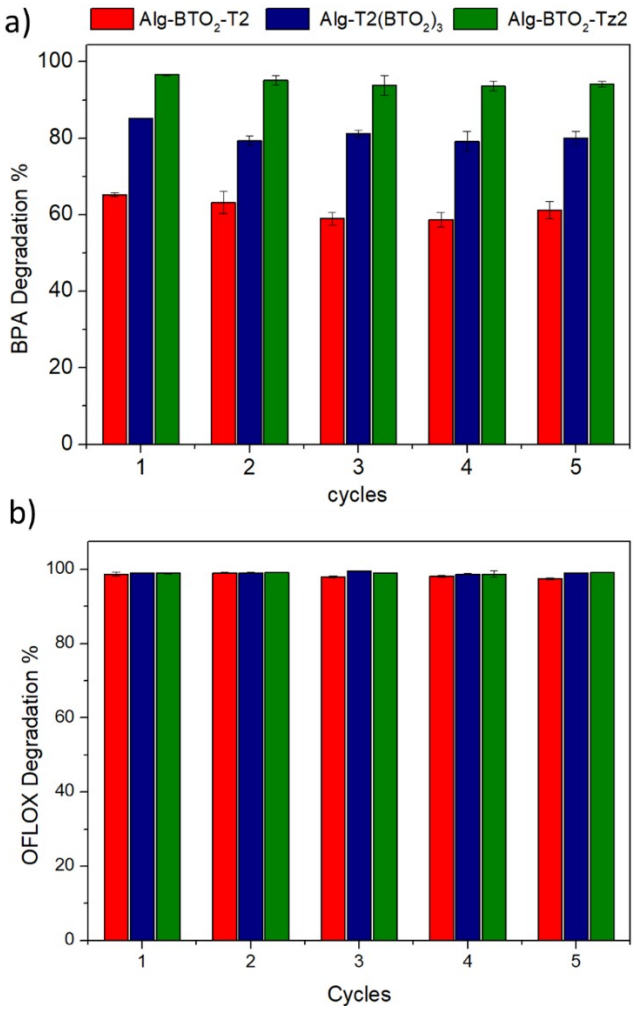

Figure S9. Recycle of Alg-BTO_2-T2, Alg-T2$(BTO_2)_3$ and Alg-BTO_2-Tz2 aerogels on a) BPA, b) OFLOX (V = 3 mL, C_{IN} = 4 mg/L, 5 mg of photocatalysts).

5. High performance liquid chromatography analyses

HPLC analyses of photodegradation samples were performed on a Shimadzu Nexera XR UHPLC system equipped with a LC-40D XR pump, a SIL-40C XR autosempler, a DGU-405 degassing unit, a CTO-40S column oven and a SPD-M40 photodiode array (PDA) detector. 200 µL samples were used as source for the automated injection. The chromatographic separation was performed on a Zorbax Eclipse XDB-C18 column (4.6 × 150 mm, 5 µm) at flow rate 1.0 mL/min, detection at λ_{max} of each analyte, linear gradient trifluoroacetic acid 0.1% aqueous solution/methanol from 90:10 to 40:60. In each experiment, the removal of each analyte was determined by comparison with that of the initial untreated solution. The results are expressed as the mean of two independent experiments ± standard deviation.

6. Ecotoxicity experiments

Aliivibrio fischeri bacteria (strain NRRL B-11177) was used and the standardized acute bioassay was performed,[19] to assess the toxicity of the various ofloxacin solutions. This method provides signal of acute toxicity based on the reduction of bioluminescence naturally emitted by the *A. fischeri*, in contact with contaminants in solution. Bioluminescence was measured ($\lambda \leq 490$ nm) using the luminometer Microtox® analyser (Model 500, Modern Water, UK).

Bioassays were performed using freeze-dried bacteria (batch number BL11251022) purchased from Ecotox LDS s.r.l. (Milan, Italy). The bioassay method consists on put rehydrated bacteria in contact with samples, a negative (saline solution: 20 g/L NaCl) and positive (reference toxicant: 3,5-dichlorophenol) control. The pH of all samples was measured and corrected with a solution of HCl (0.1 M) or NaOH (0.1 M), to obtain values between 6.0 and 8.0. All bioassays were performed in triplicate and the Coefficient of Variation (CV%: standard deviation/mean × 100) was verified (CV>20%) for each trial (Persoone et al., 2003; Environment Canada, 2007). The effects were calculated using the Microtox calculation software (Microtox Omni® software V 4.2).

The solutions (in ultrapure water) analysed were: OFLOX (C_{IN} = 4 mg/L); OFLOX (C_{IN} = 4 mg/L) irradiated with blue visible light (λ_{em} = 461 nm, irradiation power density = 10 mW/cm^2, distance about 10 cm) for 5 h; OFLOX (C_{IN} = 4 mg/L) irradiated with blue visible light (λ_{em} = 461 nm, irradiation power density = 10 mW/cm^2, distance about 10 cm) for 5 h in the presence of Alg-BTO_2-T2 (20 mg in a total volume of 12 mL); Alg-BTO_2-T2 dispersed in ultrapure water (20 mg in a total volume of 12 mL); Alg-BTO_2-T2 dispersed in ultrapure water (20 mg in a total volume of 12 mL) irradiated with blue visible light (λ_{em} = 461 nm, irradiation power density = 10 mW/cm^2, distance about 10 cm).

Table S4. Ecotoxicity of ofloxacin solutions, exposed to *Aliivibrio fischer*i for 5, 15, 30 minutes. Effect %: mean value of bioluminescence inhibition; s.e.: standard error.

	5 min		***15 min***		***30 min***	
Solution	***effect %***	***s.e.***	***effect %***	***s.e.***	***effect %***	***s.e.***
OFLOX	2.28	0.23	0.32	0.32	6.91	1.23
OFLOX + UV	7.96	0.69	3.45	0.82	9.30	2.01
OFLOX+BTO_2-T2+UV	13.60	1.39	6.27	0.72	0.93	0.42
BTO_2-T2	6.20	1.41	2.40	1.39	0.20	0.20
BTO_2-T2+UV	12.68	0.96	11.13	1.69	10.86	1.65

7. References

1. Barbarella, G.; Favaretto, L.; Sotgiu, G.; Zambianchi, M.; Fattori, V.; Cocchi, M.; Cacialli, F.; Gigli, G.; Cingolani, R., Modified Oligothiophenes with High Photo- and Electroluminescence Efficiencies. *Advanced Materials* **1999,** *11* (16), 1375-1379.
2. Barbarella, G.; Favaretto, L.; Zanelli, A.; Gigli, G.; Mazzeo, M.; Anni, M.; Bongini, A., V-Shaped Thiophene-Based Oligomers with Improved Electroluminescence Properties. *Advanced Functional Materials* **2005,** *15*, 664-670.
3. Shimotani, H.; Ikeda, S.; Asao, N.; Yamamoto, Y.; Tanigakiab, K.; Jin, T., Biphenyl end-capped bithiazole co-oligomers for high performance organic thin film field effect transistors1. *Chemical Communications* **2016,** *52*, 4926-4929.
4. Hassan, J.; Lavenot, L.; Gozzi, C.; Lemaire, M., A convenient catalytic route to symmetrical functionalized bithiophenes. *Tetrahedron Letters* **1999,** *40* (5), 857-858.
5. Frisch, M. J. T., G. W.; Schlegel, H. B.; Scuseria, G. E.; Robb, M. A.; Cheeseman, J. R.; Scalmani, G.; Barone, V. . M.; B.; Petersson, G. A.; Nakatsuji, H.; Caricato, M.; Li, X.; Hratchian, H. P.; Izmaylov, A. F.; Bloino, J.; Zheng, G.; Sonnenberg, J. L.; Hada, M. .; Ehara, M.; Toyota, K.; Fukuda, R.; Hasegawa, J.; Ishida, M.; Nakajima, T.; Honda, Y.; Kitao, O.; Nakai, H.; Vreven, T.; Montgomery, Jr., J. A. .; Peralta, J. E.; Ogliaro, F.; Bearpark, M. J.; Heyd, J.; Brothers, E. N.; Kudin, K. N.; Staroverov, V. N.; Kobayashi, R.; Normand, J. .; Raghavachari, K.; Rendell, A. P.; Burant, J. C.; Iyengar, S. S.; Tomasi, J.; Cossi, M.; Rega, N.; Millam, N. J.; Klene, M.; Knox, J. E.; Cross, J. B.; Bakken, V.; Adamo, C.; Jaramillo, J.; Gomperts, R. .; Stratmann, R. E.; Yazyev, O.; Austin, A. J.; Cammi, R.; Pomelli, C.;Ochterski, J. W.; Martin, R. L.; Morokuma, K.; Zakrzewski, V. G. .; Voth, G. A.; Salvador, P.; Dannenberg, J. J.; Dapprich, S.; Daniels, A.; D.; Farkas, O.; Foresman, J. B.; Ortiz, J. V.; Cioslowski, J.; Fox, D. J. , Gaussian16 (Revision A.03). *Gaussian16, Wallingford, CT* **2016**.
6. Cossi, M.; Barone, V.; Cammi, R.; Tomasi, J., Ab initio study of solvated molecules: a new implementation of the polarizable continuum model. *Chemical Physics Letters* **1996,** *255* (4), 327-335.
7. Yanai, T.; Tew, D. P.; Handy, N. C., A new hybrid exchange–correlation functional using the Coulomb-attenuating method (CAM-B3LYP). *Chemical Physics Letters* **2004,** *393* (1), 51-57.
8. Canola, S.; Mardegan, L.; Bergamini, G.; Villa, M.; Acocella, A.; Zangoli, M.; Ravotto, L.; Vinogradov, S. A.; Di Maria, F.; Ceroni, P., One-and two-photon absorption properties of quadrupolar thiophene-based dyes with acceptors of varying strengths. *Photochemical Photobiological Sciences* **2019,** *18*, 2180-2190.
9. Cantelli, A.; Malferrari, M.; Soldà, A.; Simonetti, G.; Forni, S.; Toscanella, E.; Mattioli, E. J.; Zerbetto, F.; Zanelli, A.; Di Giosia, M.; Zangoli, M.; Barbarella, G.; Rapino, S.; Di Maria, F.; Calvaresi, M., Human Serum Albumin–Oligothiophene Bioconjugate: A Phototheranostic Platform for Localized Killing of Cancer Cells by Precise Light Activation. *JACS Au* **2021,** *1* (7), 925-935.
10. Turrini, E.; Ulfo, L.; Costantini, P. E.; Saporetti, R.; Di Giosia, M.; Nigro, M.; Petrosino, A.; Pappagallo, L.; Kaltenbrunner, A.; Cantelli, A.; Pellicioni, V.; Catanzaro, E.; Fimognari, C.; Calvaresi, M.; Danielli, A., Molecular engineering of a spheroid-penetrating phage nanovector for photodynamic treatment of colon cancer cells. *Cellular and Molecular Life Sciences* **2024,** *81* (1), 144.
11. Petrosino, A.; Saporetti, R.; Starinieri, F.; Sarti, E.; Ulfo, L.; Boselli, L.; Cantelli, A.; Morini, A.; Zadran, S. K.; Zuccheri, G., A modular phage vector platform for targeted photodynamic therapy of Gram-negative bacterial pathogens. *iScience* **2023,** *26* (10).
12. Bortot, B.; Apollonio, M.; Baj, G.; Andolfi, L.; Zupin, L.; Crovella, S.; di Giosia, M.; Cantelli, A.; Saporetti, R.; Ulfo, L.; Petrosino, A.; Di Lorenzo, G.; Romano, F.; Ricci, G.; Mongiat, M.; Danielli, A.; Calvaresi, M.; Biffi, S., Advanced photodynamic therapy with an engineered M13 phage targeting EGFR: Mitochondrial localization and autophagy induction in ovarian cancer cell lines. *Free Radical Biology and Medicine* **2022,** *179*, 242-251.

13. Ulfo, L.; Cantelli, A.; Petrosino, A.; Costantini, P. E.; Nigro, M.; Starinieri, F.; Turrini, E.; Zadran, S. K.; Zuccheri, G.; Saporetti, R., Orthogonal nanoarchitectonics of M13 phage for receptor targeted anticancer photodynamic therapy. *Nanoscale* **2022,** *14* (3), 632-641.
14. Di Sante, M.; Kaltenbrunner, A.; Lombardo, M.; Danielli, A.; Costantini, P. E.; Di Giosia, M.; Calvaresi, M., Putting a "C60 Ball" and Chain to Chlorin e6 Improves Its Cellular Uptake and Photodynamic Performances. *Pharmaceuticals* **2023,** *16* (9), 1329.
15. Marconi, A.; Giugliano, G.; Di Giosia, M.; Marforio, T. D.; Trivini, M.; Turrini, E.; Fimognari, C.; Zerbetto, F.; Mattioli, E. J.; Calvaresi, M., Identification of blood transport proteins to carry temoporfin: a domino approach from virtual screening to synthesis and in vitro PDT testing. *Pharmaceutics* **2023,** *15* (3), 919.
16. Greco, G.; Ulfo, L.; Turrini, E.; Marconi, A.; Costantini, P. E.; Marforio, T. D.; Mattioli, E. J.; Di Giosia, M.; Danielli, A.; Fimognari, C., Light-enhanced cytotoxicity of doxorubicin by photoactivation. *Cells* **2023,** *12* (3), 392.
17. Mattioli, E. J.; Ulfo, L.; Marconi, A.; Pellicioni, V.; Costantini, P. E.; Marforio, T. D.; Di Giosia, M.; Danielli, A.; Fimognari, C.; Turrini, E., Carrying temoporfin with human serum albumin: A new perspective for photodynamic application in head and neck cancer. *Biomolecules* **2022,** *13* (1), 68.
18. Tunioli, F.; Khaliha, S.; Mantovani, S.; Bianchi, A.; Kovtun, A.; Xia, Z.; Bafqi, M. S. S.; Okan, B. S.; Marforio, T. D.; Calvaresi, M.; Palermo, V.; Navacchia, M. L.; Melucci, M., Adsorption of emerging contaminants by graphene related materials and their alginate composite hydrogels. *Journal of Environmental Chemical Engineering* **2023,** *11* (2), 109566.
19. UNI EN ISO (2019) UNI EN ISO 11348-3:2019. Water quality - Determination of the inhibitory effect of water samples on the light emission of Vibrio fischeri (Luminescent bacteria test) - Part 3: Method using freeze-dried bacteria.